On sinterability of nanostructured W produced by high-energy ball milling

R. Malewar
Defense Metallurgical Research Laboratory, Hyderabad, India

K.S. Kumar
Department of Metallurgical and Materials Engineering, Indian Institute of Technology, Kharagpur 721302, India

B.S. Murty
Department of Metallurgical and Materials Engineering, Indian Institute of Technology, Madras, Chennai 600036, India

B. Sarma
Defense Metallurgical Research Laboratory, Hyderabad, India

S.K. Pabi[a)]
Department of Metallurgical and Materials Engineering, Indian Institute of Technology, Kharagpur 721302, India

(Received 31 May 2006; accepted 18 September 2006)

The present investigation reports for the first time a dramatic decrease in the sintering temperature of elemental W from the conventional temperature of ⩾2500 °C to the modest temperature range of 1700–1790 °C by making the W powder nanostructured through high-energy mechanical milling (MM) prior to sintering. The crystallite size of the initial W powder charge with a particle size of 3–4 μm could be brought down to 8 nm by MM for 5 h in WC grinding media. Further milling resulted in a high level of WC contamination, which apparently was due to work hardening and the grain refinement of W. A sintered density as high as 97.4% was achieved by sintering cold, isostatically pressed nanocrystalline (8 nm) W powder at 1790 °C for 900 min. The microstructure of the sintered rods showed the presence of deformation bands, but no cracks, within a large number of W grains. The mechanical properties, when compared with the hardness and elastic modulus, of the sintered nano-W specimen were somewhat superior to those reported for the conventional sintered W.

I. INTRODUCTION

Tungsten can be an excellent high-temperature structural material for applications in temperatures up to 2480 °C because of its attractive properties, compared to a high melting point of 3420 °C, a density of 19.3 g/ml, a hardness of 9.75 GPa, an elastic modulus of 407 GPa, a low coefficient of thermal expansion, good thermal conductivity, and low vapor pressure.[1] However, the consolidation of a conventional microcrystalline W powder with an average particle size of 3–4 μm is difficult,[2–5] and normally electrical resistance sintering under hydrogen atmosphere at temperatures of 2500 °C or more is used for this purpose.[4–8] The process is expensive and usually only simple shapes like filaments, rods, or bars are sintered by this method.

Several studies have shown that the onset of sintering can take place at a significantly lower temperature in the case of nanoparticles compared to conventional microcrystalline powders.[9–15] For instance, the sintering of both metals and ceramic nanoparticles was found to start at temperatures of 0.2–0.4 T_m (T_m = melting temperature) compared to 0.5–0.8 T_m for the conventional powders. It is believed that in the case of nanostructured powders the grain boundary sliding, dislocation motion, grain rotation, and viscous flow can significantly contribute to the enhanced sintering kinetics.[11–15] An investigation of the effects of nanostructure formation on the sinterability of W powder is yet to be reported; hence, this has been attempted in the present investigation. This work is of particular interest for fabricating structural components of intricate shape for very high-temperature applications.

[a)]Address all correspondence to this author.
e-mail: skpabi@metal.iitkgp.ernet.in
DOI: 10.1557/JMR.2007.0166

Information on the nanostructure formation in elemental W by high-energy mechanical milling (MM) in tungsten carbide grinding media is not available in the literature, to the best of our knowledge; hence, this process for W has also been investigated here. In an earlier study, Ricceri and Matteazzi[16] reported on the production of nanostructured W powder by a chemical-mechanical synthesis method; but, they did not report any results of the sintering of these powders. The present article reports for the first time the results of compaction and sintering of mechanically milled, nanostructured W.

II. EXPERIMENTAL

A planetary ball mill (Fritsch Pulverisette P5, Idar-Oberstein, Germany) was used to mechanically mill an elemental W powder with a particle size of 3–4 μm (99.95% purity) at a mill speed of 300 revolutions per minute using WC grinding media and maintaining a ball-to-powder weight ratio of 10:1. Milled samples were taken out at predetermined intervals for their characterization.

A high-resolution x-ray diffractometer (X'pert Pro; Philips, Amsterdam, The Netherlands) was used for recording the x-ray diffraction (XRD) patterns of powder and sintered specimens. A rough estimate of WC contamination in some milled samples was obtained by comparing the integrated intensities of W_{110} and WC_{100} peaks, and assuming that the R-factors for both of the reflections were identical.[17] Crystallite size and root mean square (rms) strain in the ball-milled samples were calculated from the XRD line broadening using the equation[18–20]:

$$B\cos(\theta) = (0.94\,\lambda)/d + \epsilon\sin(\theta) \quad , \qquad (1)$$

where, d is crystal size, ϵ is the rms strain, and B is the full-width at half-maximum (FWHM) exclusively due to crystallite size and rms strain. The peak broadening due to factors other than those from MM was eliminated as

$$B^2 = B^2_{\mathrm{M}} - B^2_{\mathrm{S}} \quad , \qquad (2)$$

where, B_{S} and B_{M} are the FWHM of any particular reflection from the annealed powder and milled powder, respectively. Refined values of the lattice parameter (a) were calculated from peak positions in the XRD pattern by the extrapolation of a against the term $\cos^2\theta/\sin\theta$ to $\cos\theta = 0$.[17] Some powder samples were examined using a Philips CM12 transmission electron microscope (TEM) or a JEOL (Tokyo, Japan) JSM5800 scanning electron microscope (SEM) fitted with an energy-dispersive x-ray (EDX) microanalysis attachment.

Pure W powder was ball milled for 5 h with a view to making it nanostructured without any significant contamination (see Sec. III), and then it is compacted by a cold isostatic press (Make; National Forge, Temse, Belgium) under a hydrostatic pressure of 350 MPa to produce cylindrical rods of 15–20 mm diameter with a length varying from 80 to 120 mm. Green compacts were sintered under flowing hydrogen atmosphere at 1300, 1700, and 1790 °C for up to 900 min. Sintered densities were evaluated by the Archimedes principle using the Sartorius density measurement kit (Göttingen, Germany).

Murakami reagent was used as the etchant to develop the microstructure of sintered W. A Leica (Leitz, Oberkochen, Germany) high-resolution optical microscope with differential interference contrast (DIC) and a charge-coupled device camera was used to observe the microstructure of the tungsten grains and the presence of any crack or other phases. The Leica QWIN image-processing software interfaced with the microscope was used to estimate the area fraction of selected constituents in the micrographs. The mechanical properties, compared with the hardness and elastic modulus, were determined by an MTS nanoindenter (West Sacramento, CA) in continuous stiffness measuring mode with a limit of the indentation depth set at 2000 nm.

III. RESULTS AND DISCUSSION

The SEM micrograph in Fig. 1 illustrates the nearly equiaxed morphology of the W powder, with a particle size of 3–4 μm, which was used for the MM. The XRD patterns of the milled W at different milling times (Fig. 2) showed continuous broadening of the peaks, thus evidencing the refinement of the W crystallite size by ball milling. The crystallite size of W, which was calculated from these XRD patterns, diminished to 8 nm after 5 h of milling (Fig. 3). The dark-field TEM image of the as-milled powder in Fig. 4 reveals the W crystallite size after 5 h of milling, and it is in reasonable agreement with results of the XRD analysis. Ball milling beyond 5 h up to 15 h seems to increase the crystallite size from 8 to 14 nm (Fig. 3), and a qualitatively similar feature has also been observed during the ball milling of a few other systems like Cu–Zn[21] and Ni–Al–Cr.[22] During the MM operation, nanocrystals form through repeated cold

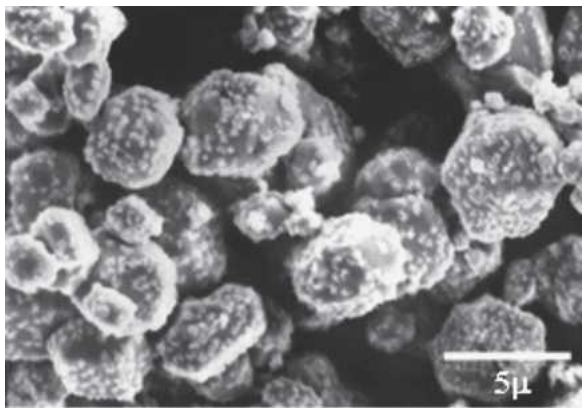

FIG. 1. SEM image of the as-received W powder.

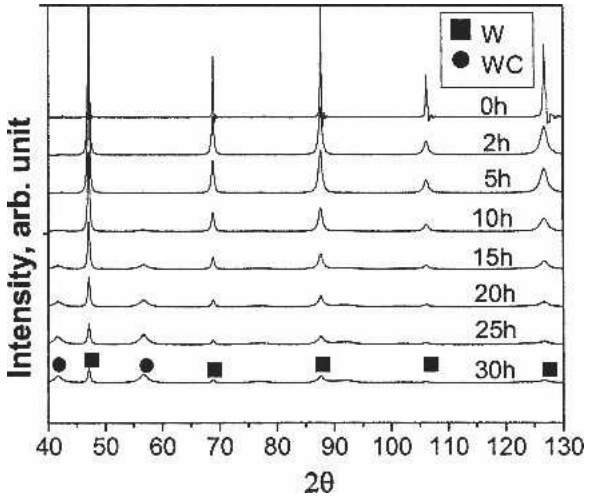

FIG. 2. XRD patterns of W powder as a function of MM time.

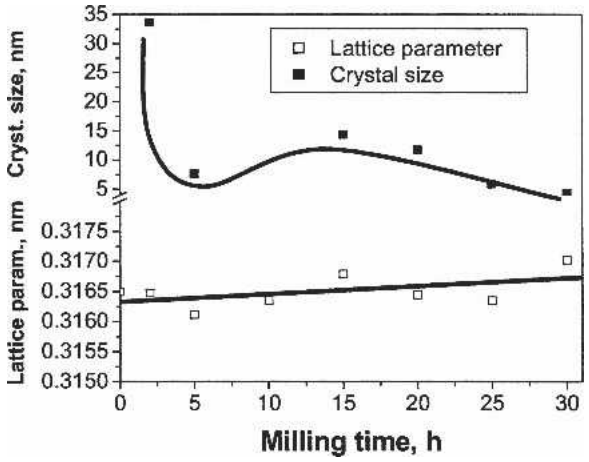

FIG. 3. Variations of crystal size and lattice parameter of W with milling time.

welding and the fracture of powder particles[23]; if the welding process dominates over the fracture at some stage of MM, some increase in the crystal size at that time is plausible. However, beyond 20 h of milling there was only a marginal decrease in the crystal size of W.

The variation of the lattice parameter of W with milling time is also displayed in Fig. 3, which shows a monotonic and marginal increase up to 0.28% after 30 h of milling, apparently due to the negative hydrostatic pressure experienced by the nanocrystals,[24] even though the possibility of the dissolution of some C in W is not ruled out. However, it may be pointed out that more pronounced lattice expansion has been observed during the ball milling of other metallic systems like Nb and $Nb_{80}Al_{20}$[25–28] or $Ni_{90}Si_{10}$.[29] Moreover, positron lifetime measurements in Nb evidenced a sharp increase in the free volume in the grain boundaries during milling especially with grain sizes below 10 nm, and this was expected to exert a negative hydrostatic pressure on the

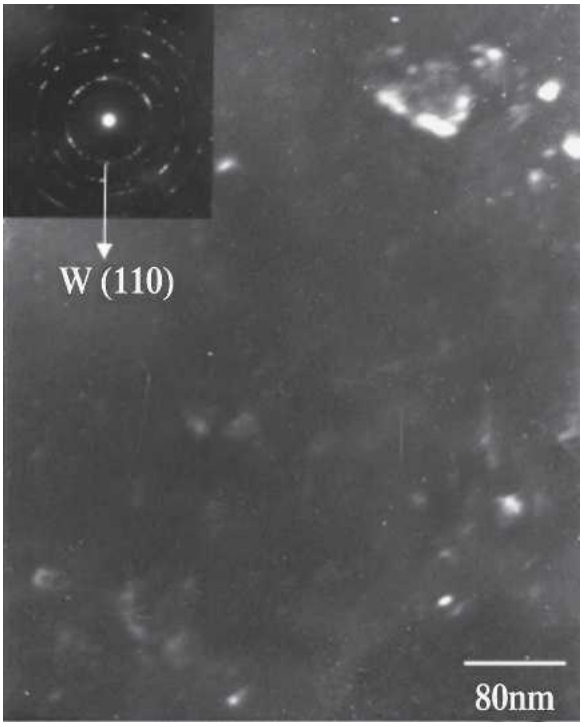

FIG. 4. Dark-field TEM image of W powder milled for 5 h revealing suitably oriented crystallites as bright regions. The electron diffraction pattern of this nanostructured powder in the inset displays the typical ring pattern of W.

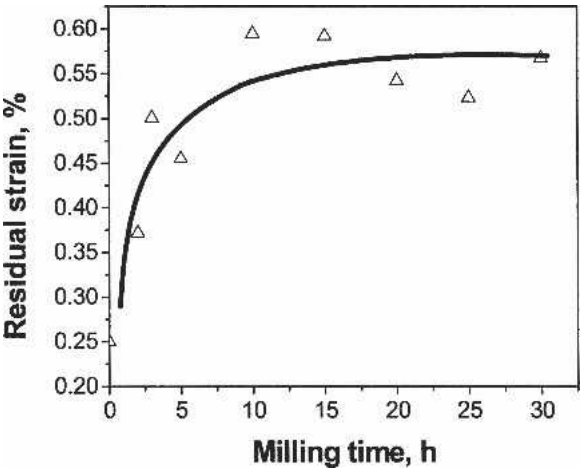

FIG. 5. Variation of the rms strain of W with milling time.

adjacent lattice, resulting in lattice expansion.[26,27] Dissolved interstitials in Nb, if any, could not account for the observed free volume increase.

The root mean square (rms) strain of the W powder initially increased with milling time to reach a saturation level of about 0.6% after about 10 h of milling (Fig. 5). Figure 2 shows contamination by WC grinding media after 15 h of milling. The extent of WC contamination, which was calculated from the XRD patterns, is shown in Fig. 6, which shows a steep increase in the WC

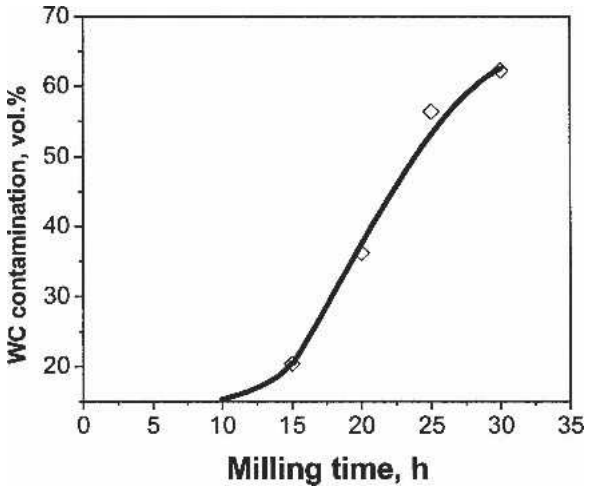

FIG. 6. Extent of WC contamination during MM of W up to 30 h.

contamination level after 15 h and reaching about 60 vol% after 30 h of MM. The hardness of the WC vial and balls (13–16 GPa[30]) is known to be much higher than the conventional microcrystalline W (9.7 GPa).[1] The high level of contamination by WC milling media after the W became nanostructured by ball milling suggests that the hardness of the W nanoparticles produced by MM becomes comparable to that of the WC grinding media, and that it can be attributed to the rapid work hardening of W below its transition temperature (i.e., >650 K)[1,31] and the increase in the yield strength of fine-grained W due to the Hall–Petch effect.[18]

To minimize the WC contamination from the milling media in the nanostructured W powder, which is to be used for subsequent compaction and sintering, the duration of MM in the ensuing experiments was restricted to 5 h. At this stage of milling, no WC contamination in the W powder was detectable by XRD (Fig. 2), although the EDX pattern in Fig. 7(a) reveals the presence of traces of C and O. This short milling duration (i.e., 5 h) was also advantageous for generating a substantial quantity of nanostructured powder with the laboratory ball mill (Pulverisette P5; Fritsch). The compaction property of this nanostructured W powder was rather poor, and it resulted in only 57% green densification in cold isostatically pressed compacts with a diameter of 15 mm. The variation of the sintered density of nanocrystalline (8 nm) tungsten with time at 1300, 1700, and 1790 °C is displayed in Fig. 8. The sintered density of 83.2% was obtained after 600 min at 1300 °C, and it can be regarded as a very significant extent of densification for pure W at a relatively low temperature, because conventional microcrystalline W is normally sintered at 2500 °C or above.[4–7] Interestingly, when the cold, isostatically pressed, nanostructured (8 nm) W powder compacts were sintered at 1700 °C, a sintered density of 93.2% was achieved after 320 min of sintering.

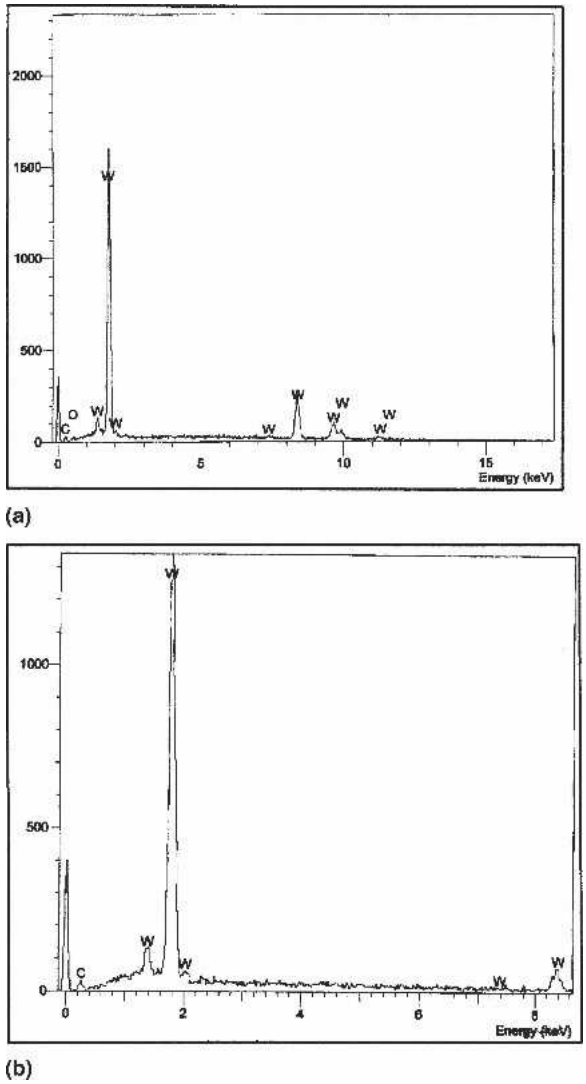

FIG. 7. EDX spectrum of W (a) after MM for 5 h, resulting in a nanostructured powder, and (b) after its subsequent sintering at 1700 °C. Traces of C and O are evident in (a), whereas only a trace of C is present in (b).

The optical micrograph of the unetched W specimen sintered at 1700 °C for 320 min in the DIC inverse contrast mode is displayed in Fig. 9(a), and that after etching is shown in Fig. 9(b). The image processing of the unetched micrographs [as in Fig. 9(a)] yielded the presence of 2–3% pores (P), and these were visible by light microscopy as protruded regions due to inverse contrast. The etched microstructures of the same specimen revealed 5–6% pores, which agreed well with the macroscopic sintered density measurements (93.2%). The grains in this specimen were 6–10 μm in size. The XRD pattern of the sintered specimen inserted in Fig. 9(b) shows the presence of W crystals only. However, the EDX spectrum of this specimen in Fig. 7(b) shows the presence of traces of C and no oxygen.

An increase in the sintering temperature to 1790 °C

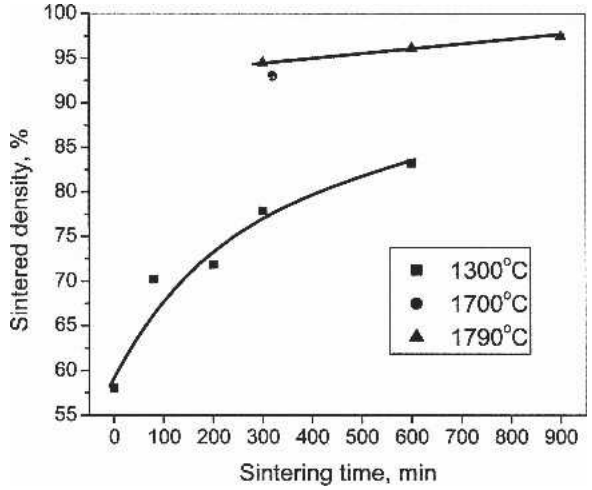

FIG. 8. Sinterability of W at 1300, 1700, and 1790 °C.

enabled attainment of a density of 97.4% after sintering the nanocrystalline W powder for 900 min (Fig. 8). This remarkable densification can be attributed to the nanostructure and strain-induced defects in the W powder used for the sintering process.[13–15,18] However, despite the many investigations carried out in the last fifteen years or more, the mechanism of the enhanced sintering of nanostructured powders is not well understood, and the topic has been dealt with extensively in some recent reviews.[14,15] Molecular dynamic simulations of the nanosized powders have indicated an extremely fast sintering behavior,[12,32] and the surface diffusion cannot account for this. Here, generally in the initial stage of sintering, processes like grain boundary slip, dislocation motion, grain rotation, and viscous flow can play a significant role.[15] In the case of nanostructured W, however, the high sintering temperature precluded the experimental identification/observation of these processes.

The microstructure of the etched W specimen sintered at 1790 °C for 900 min is shown in Fig. 9(c). The grain size in this sintered W rod was relatively coarse and varied from 15–30 μm, compared to a grain size of 6–10 μm after sintering nanostructured W for 320 min at 1700 °C [Fig. 9(b)]. The DIC image indicated the presence of slip bands (SB) in many W grains [e.g., in Fig. 9(c)] as a signature of the extensive deformation of W grains during prior milling. No cracks were visible even at a magnification of 2500× in the DIC mode, suggesting that the sample got uniformly densified at 1700 or 1790 °C.

The hardness and the elastic modulus of the nanocrystalline W sintered at 1700 °C to 93.2% density and a grain size of 6–10 μm were measured by the nanoindenter; the results are shown in Fig. 10. The average hardness of W grains was 12.6 GPa, which is higher than that of the microcrystalline W (9.7 GPa) reported in the literature.[1–3] The average elastic modulus of

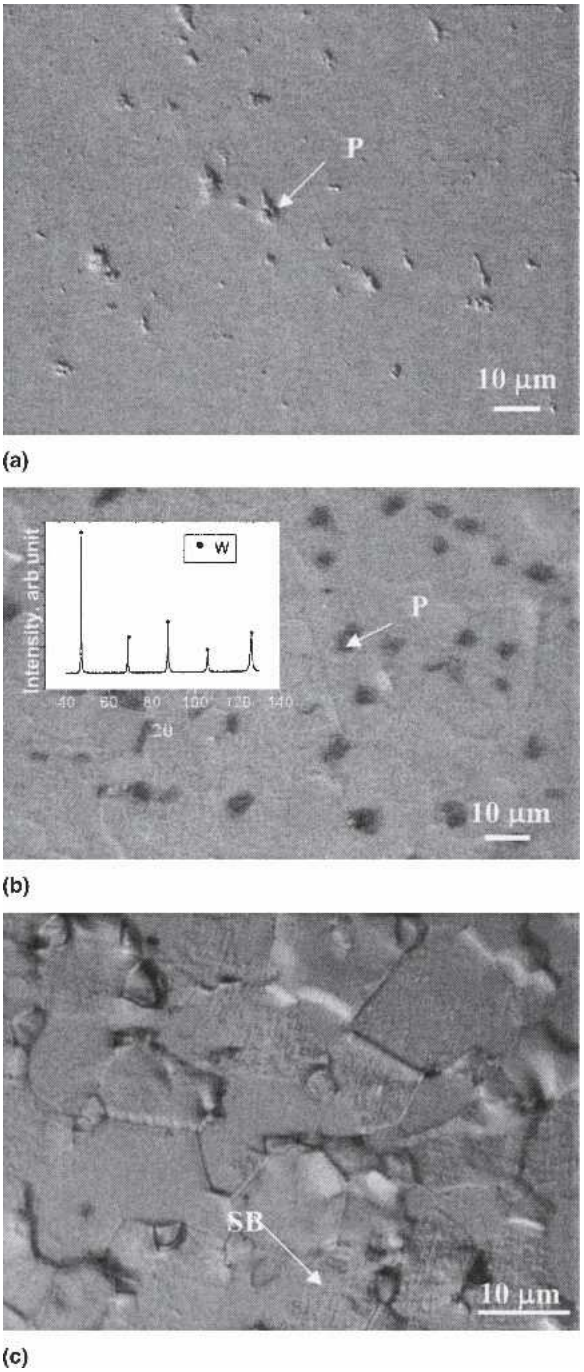

FIG. 9. Microstructure of sintered W in DIC mode: (a) unetched and (b) etched specimen sintered at 1700 °C for 320 min. The inset in (b) is the diffraction pattern from this specimen, showing the presence of W only. (c) DIC microstructure of W sintered at 1790 °C for 900 min and etched.

nanocrystalline W sintered at 1700 °C was 490 GPa, which is also higher than that of conventional microcrystalline W (411 GPa).[2,3] This apparent improvement in the mechanical properties of nanocrystalline W sintered at 1700 °C may be related to the large number of fine and deformed tungsten grains.

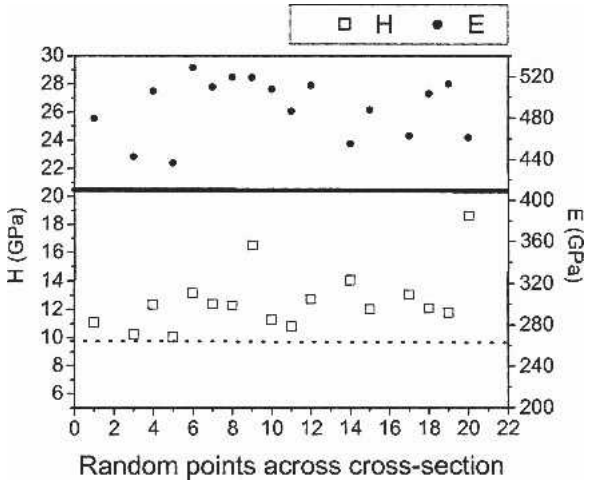

FIG. 10. Nanoindentation hardness (H) and elastic modulus (E) of W sintered at 1700 °C for 320 min. Corresponding values of H and E for microcrystalline W reported in the literature[1–3] are shown by dotted and solid bold lines, respectively.

The reduction in the sintering temperature of W by making it nanostructured was expected from similar studies on other materials.[9–15] However, the effect in the present case is rather dramatic. The ability to sinter W at 1700 °C will make the fabrication of high-temperature structural components with complex geometry much easier. The enhanced densification significantly depends on the crystal size reduction, the production of nonagglomerated particles, and the lack of oxide contamination on the particles.[14,15] The present MM conditions appear to be quite effective in this regard. The grain growth accompanying the present sintering process was not unexpected, because the pressureless sintering method used in the present study is normally not able to retain the nanosize in the sintered product.[13–15] Nevertheless, the reduction of the sintering temperature of W to 1700–1790 °C can make the commercial fabrication of W products for high-temperature applications much easier, when compared to that achieved by the conventional sintering process at temperatures ⩾2500 °C.

IV. CONCLUSIONS

The crystallite size of elemental W could be brought down to 8 nm by high-energy MM in WC grinding media within 5 h of milling; but a further increase in milling time caused a very significant increase in WC contamination from milling media, apparently due to the grain refinement and strain hardening of W. Interestingly, from a green density of 57% in cold, isostatically pressed compacts a sinter density as high as 97.4% could be achieved by sintering at 1790 °C for 900 min, which is much lower than the conventional sintering temperature of ⩾2500 °C used by the electrical resistance heating for the microcrystalline W powder, which is a fact of profound technological interest. The sample sintered at 1700 °C had a grain size of 6–10 μm, and it showed higher hardness and elastic modulus compared to the conventionally sintered W.

ACKNOWLEDGMENTS

The work was sponsored by the Department of Science and Technology, Government of India through Grant No. SR/S5/NM-91/2002 and by the Defense Research and Development Organization, Government of India through Grant No. ERIP/ER/0100169/M/01. One of the authors (R. Malewar) gratefully acknowledges the financial support of the Ministry of Defense. The authors are grateful to Prof. S. Das, Prof. K. Das, and Mr. S. Nayek of the Metallurgical and Materials Engineering Department, Indian Institute of Technology, Kharagpur, for many stimulating discussions.

REFERENCES

1. W.F. Smith: *Structure and Properties of Engineering Alloys*, 2nd ed. (McGraw Hill, New York, NY, 1993), pp. 580–586.
2. M. Trazaska: Correlation between the temperature distribution and the structure of resistance sintered tungsten bars. *Int. J. Refract. Met. Hard Mater.* **14,** 235 (1996).
3. L. Uray: AKS doped tungsten investigated by electrical resistivity: I. Manufacturing tungsten bar and wire. *Int. J. Refract. Met. Hard Mater.* **20,** 311 (2002).
4. L. Uray: AKS doped tungsten wire investigated by electrical measurements: II. Impurities in tungsten. *Int. J. Refract. Met. Hard Mater.* **20,** 319 (2002).
5. A. Grüger, R. Vassen, and F. Mertens: The evaporation of potassium during sintering of doped tungsten. *Int. J. Refract. Met. Hard Mater.* **16,** 37 (1998).
6. Z. Kolczynski, W. Rutkowski, M.B. Swierczynska, and M. Trzanska: Structure of sintered tungsten bars as effect of processing load. *Powder Metall. Int.* **20,** 22 (1988).
7. E. Pink and L. Bartha: *The Metallurgy of Doped/Non-Sag Tungsten* (Elsevier, New York, NY, 1989), pp. 127–135.
8. M. Trzaska: Influence of technological parameters on the structure of tungsten sintered bars. *Inz. Materialowa* **65,** 139 (1991).
9. T. Rabe and R. Wäsche: Sintering behaviour of nanocrystalline titanium nitride powders. *Nanostruct. Mater.* **6,** 357 (1995).
10. A. Pechenik, G.J. Piermarini, and S.C. Danforth: Fabrication of transparent silicon nitride from nanosize particles. *J. Am. Ceram. Soc.* **75,** 3283 (1992).
11. H. Hahn: Microstructure and properties of nanostructured oxides. *Nanostruct. Mater.* **2,** 251 (1993).
12. R.S. Averbach, H. Zhu, R. Tao, and H.J. Hofler: Sintering of nanocrystalline materials: experiments and computer simulations, in *Synthesis and Processing of Nanocrystalline Powder*, edited by D.L. Bourell (TMS, Warrendale, PA 1996), pp. 203–216.
13. L. Bourell and J.R. Groza: Consolidation of ultra fine and nanocrystalline powder, in *ASM Handbook* **7** (American Society of Metals, Metals Park, OH, 1998), pp. 583–589.
14. J.R. Groza: Sintering of nanocrystalline powders. *Int. J. Powder Metall.* **35,** 59 (1999).
15. J.R. Groza: Nanocrystalline powder consolidation methods, in *Nanostructured Materials-Processing, Properties and Potential*

*Application*s, edited by C.C. Koch (Noyes, New York, NY, 2002), pp. 115–178.
16. R. Ricceri and P. Matteazzi: A study of formation of nanometric W by room temperature mechanosynthesis. *J. Alloys Compd.* **358,** 71 (2003).
17. B.D. Cullity: *Elements of X-Ray Diffraction*, 2nd edition (Addison Wesley, Reading, MA, 1978), pp. 350–368, 411–415.
18. C. Suryanarayana: Mechanical alloying and milling. *Prog. Mater. Sci.* **46,** 1 (2001).
19. B. Lönnberg: Characterization of milled Si_3N_4 powder using x-ray peak broadening and surface area analysis. *J. Mater. Sci.* **29,** 3224 (1994).
20. S.K. Pabi and B.S. Murty: Mechanism of mechanical alloying in Ni-Al and Cu-Zn systems. *Mater. Sci. Eng., A* **214,** 146 (1996).
21. H-J. Fecht: Thermodynamic properties and stability of grain boundaries in metals based on the universal equation of state at negative pressure. *Acta Metall. Mater.* **38,** 1927 (1990).
22. S.K. Pabi, J. Joardar, and B.S. Murty: Formation of nanocrystalline phases in Cu-Zn system during mechanical alloying. *J. Mater. Sci.* **31,** 3207 (1996).
23. S.K. Pabi, J. Joardar, I. Manna, and B.S. Murty: Nanocrystalline phases in Cu-Ni, Cu-Zn and Ni-Al systems by mechanical alloying. *Nanostruct. Mater.* **9,** 149 (1997).
24. C.C. Koch: The synthesis and structure of nanocrystalline materials produced by mechanical attrition: A review. *Nanostruct. Mater.* **2,** 109 (1993).
25. P.P. Chattopadhyay, S.K. Pabi, and I. Manna: An allotropic transformation in Nb induced by planetary ball milling. *Mater. Sci. Eng., A* **304–306,** 424 (2001).
26. P.P. Chattopadhyay, P.M.G. Nambissan, S.K. Pabi, and I. Manna: Polymorphic transformation and lattice expansion in nanocrystalline niobium revealed by positron annihilation. *Appl. Surf. Sci.* **182,** 308 (2001).
27. P.P. Chattopadhyay, P.M.G. Nambission, S.K. Pabi, and I. Manna: Polymorphic bcc to fcc transformation of nanocrystalline niobium studied by positron annihilation. *Phys. Rev. B: Condens. Matter* **63,** 54107 (2001).
28. P.P. Chatterjee, S.K. Pabi, and I. Manna: An allotropic transformation induced by mechanical alloying. *J. Appl. Phys.* **86,** 5912 (1999).
29. M.K. Datta, S.K. Pabi, and B.S. Murty: Phase fields in nickel silicides obtained by mechanical alloying. *J. Appl. Phys.* **87,** 8393 (2000).
30. S. Berger, R. Porat, and R. Rosen: Nanocrystalline materials: A study of WC-based hard metals. *Prog. Mater. Sci.* **42,** 311 (1997).
31. D. Brunner: Peculiarities of work hardening of high-purity tungsten single crystals below 800 K. *Mater. Sci. Eng., A* **387–389,** 167 (2004).
32. H. Zhu and R.S. Averbech: Sintering processes of two nanoparticles: A study by molecular dynamics simulations. *Philos. Mag. Lett.* **73,** 27 (1996).